Digital Communications and Networks 4 (2018) 98–105

Contents lists available at ScienceDirect

Digital Communications and Networks

journal homepage: www.keaipublishing.com/en/journals/digital-communications-and-networks/

Piecewise linear detection for direct superposition modulation

Martin Damrath *, Peter Adam Hoeher, Gilbert J.M. Forkel

Institute of Electrical and Information Engineering, Faculty of Engineering, University of Kiel, Kaiserstr. 2, 24143 Kiel, Germany

ARTICLE INFO

Keywords:
Digital modulation
Demodulation
Detection algorithms
Linear approximation

ABSTRACT

Considering high-order digital modulation schemes, the bottleneck in consumer products is the detector rather than the modulator. The complexity of the optimal a posteriori probability (APP) detector increases exponentially with respect to the number of modulated bits per data symbol. Thus, it is necessary to develop low-complexity detection algorithms with an APP-like performance, especially when performing iterative detection, for example in conjunction with bit interleaved coded modulation. We show that a special case of superposition modulation, dubbed Direct Superposition Modulation (DSM), is particularly suitable for complexity reduction at the receiver side. As opposed to square QAM, DSM achieves capacity without active signal shaping. The main contribution is a low-cost detection algorithm for DSM, which enables iterative detection by taking a priori information into account. This algorithm exploits the approximate piecewise linear behavior of the soft outputs of an APP detector over the entire range of detector input values. A theoretical analysis and simulation results demonstrate that at least max-log APP performance can be reached, while the complexity is significantly reduced compared to classical APP detection.

1. Introduction

In the past years, an increasing demand for higher data rates is observed, particularly due to the rapid progress in the fields of mobile data and media streaming. Besides multiple antenna techniques, using high-order modulation schemes exhibits a possible bandwidth-efficient solution to meet this demand. Particularly in applications like point-to-point high-speed radio links, digital video broadcasting and in conjunction with beamforming, the Signal-to-Noise Ratio (SNR) is often large enough to serve high-order modulation schemes like 1024-QAM or 65536-QAM. However, one major limitation of high-order modulation is due to the computational complexity of the corresponding detector, particularly in low-cost consumer products. When using modern receiver structures, i.e., Bit-Interleaved Coded Modulation[1] (BICM) [1] in conjunction with Iterative Detection[2] (BICM-ID) [2], the A Posteriori Probability (APP) detector[3] implemented in probability domain [3] or in log domain [4,5] provides the conventional and optimal solution to produce soft outputs. It is well known that BICM-ID significantly outperforms classical BICM. However, for general symbol constellations the computational complexity per iteration is $\mathcal{O}(2^{N'})$, where N' is equal to the number of bits per symbol, which makes APP detection impractical for high-order modulation alphabets. (For symmetrical symbol constellations, the computational complexity may be smaller. For example, for square Quadrature Amplitude Modulation (square QAM), complexity is $\mathcal{O}(2^{N'/2})$ per quadrature component, which is still exponential.)

A common simplification of APP detection is the max-log APP approximation [5], which nevertheless also leads to an overall complexity of $\mathcal{O}(2^{N'})$. Another detection approach is using the so-called Gaussian approximation, which is of complexity $\mathcal{O}(N')$ only. This approach is well known from multiuser systems [6,7]. But as shown in [8], the Gaussian approximation leads to an error floor or fails completely when applied as a multilayer detector. Thus, new low-complexity detection algorithms with APP-like performance have to be found to enable high-order modulation schemes for practical purposes in conjunction with iterative detection.

In this article, the focus is on Direct Superposition Modulation (DSM) [9], in [10] called type-I sigma-mapper, which allows the separate processing of real and imaginary parts like classical square QAM. While square QAM is currently widely used in BICM-ID systems, DSM provides a significant potential for complexity reduction at the receiver side. In addition, DSM exhibits a capacity achieving property without active

* Corresponding author.
E-mail addresses: md@tf.uni-kiel.de (M. Damrath), ph@tf.uni-kiel.de (P.A. Hoeher), gf@tf.uni-kiel.de (G.J.M. Forkel).

[1] In BICM, channel coding and modulation are combined with a bitwise interleaver in-between.
[2] By means of iterative detection, the detector (here: the demodulator) and the channel decoder exchange extrinsic information in an iterative manner.
[3] An APP detector calculates the a posteriori probability of each info bit while taking a priori information into account.

https://doi.org/10.1016/j.dcan.2016.11.005
Received 10 May 2016; Received in revised form 20 September 2016; Accepted 21 November 2016
Available online 24 November 2016

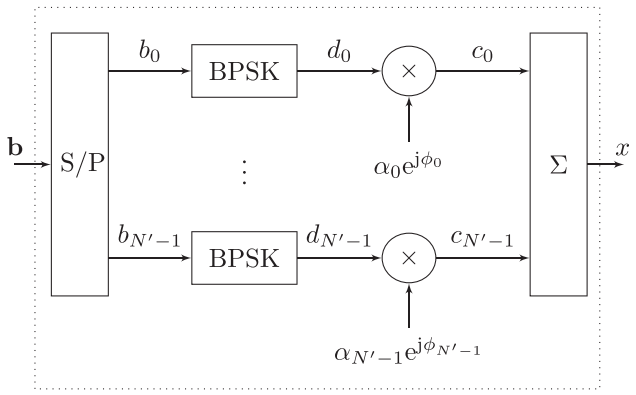

Fig. 1. Superposition modulation.

signal shaping. In this contribution, a detection algorithm is proposed, which can efficiently be implemented via Look-Up Tables (LUT), while achieving at least max-log APP performance. The algorithm is motivated by the fact that for certain modulation schemes the soft outputs of an APP detector are approximate piecewise linear over the entire range of detector input values. According to the state-of-the-art, piecewise linear detection has been applied in data transmission systems employing square QAM, assuming that no a priori information is available [11–18]. In contrast, the proposed algorithm can be applied even if a priori information is available. This fact enables modern transmitter/receiver structures like BICM-ID, which benefit from iterative detection.

The remainder of this article is organized as follows. Section 2 gives a short introduction to superposition modulation and the optimal APP detection algorithm. In Section 3 the piecewise linear approximation algorithm is presented and afterwards analyzed by simulation results in Section 4. The conclusion is finally drawn in Section 5.

2. Superposition modulation and APP detection

In Fig. 1, the general structure of Superposition Modulation (SM) is shown. In a primary step, code bits $\mathbf{b}$ are serial-to-parallel (S/P) converted into N' separate layers. Afterwards, each code bit in each layer is mapped onto a binary antipodal symbol d_n and weighted with a complex factor $a_n = \alpha_n e^{j\phi_n}$. The resulting symbols are called chips c_n. In the last step, the N' chips are simply superimposed in order to form the data symbol x:

$$x = \sum_{n=0}^{N\prime-1}(1-2b_n)a_n = \sum_{n=0}^{N\prime-1} d_n a_n = \sum_{n=0}^{N\prime-1} c_n. \tag{1}$$

The complex factors a_n can be chosen arbitrarily to construct both bijective or non-bijective constellations.[4] However, in this article the focus is on non-bijective DSM with Equal Power Allocation (EPA), because of its capacity achieving property and its potential for simplifications in the detection step. This leads to the following rule for the weighting factors:

$$a_n = \begin{cases} 1/\sqrt{N\prime} & \text{for } n \in 0,\ldots,N-1 \\ j/\sqrt{N\prime} & \text{for } n \in N,\ldots,N\prime-1 \end{cases} \tag{2}$$

where N is the number of modulated bits in the real part and $N\prime - N$ is the number of modulated bits in the imaginary part. As a result, in DSM the real and imaginary parts are modulated independently and can be demodulated separately, like in square QAM. For this reason, without loss of generality, in the remainder of this article only the real part and $\alpha = 1/\sqrt{N}$ will be considered. Hence, the corresponding symbol alphabet is

$$\mathscr{X} = [-N\alpha, -(N-2)\alpha, \ldots, (N-2)\alpha, N\alpha]. \tag{3}$$

Due to the non-bijective mapping, a combination of a suitable coding strategy and Soft-Input Soft-Output (SISO) detection[5] is essential. Hence, the symbol detector has to provide extrinsic log-likelihood ratios (LLRs) at its output. For the optimal APP detection, the extrinsic LLR of the nth bit is calculated as follows:

$$\begin{aligned} L_n &= \log\frac{p(y|b_n=0)}{p(y|b_n=1)} = \log\frac{p(y|c_n=+a_n)}{p(y|c_n=-a_n)} \\ &= \log\frac{\sum_{z\in\mathscr{Z}} P(z)p(y|z,c_n=+a_n)}{\sum_{z\in\mathscr{Z}} P(z)p(y|z,c_n=-a_n)} \end{aligned} \tag{4}$$

where $z = \sum_{i=0,i\neq n}^{N-1} c_i$ represents the interfering symbol defined over the alphabet $\mathscr{Z}$, and y is the noisy received sample (i.e., the observation) at the receiver side. It is also possible to rewrite (4) so that the sum is over all the interfering bit combinations. Anyway, in the case of DSM-EPA (4) provides the more accessible notation, because it exploits the non-bijectivity and thereby reduces the number of summands. Furthermore, the max-log APP detector can simply be implemented by replacing the sum-operations by max-operations in (4). If the sum over all interfering bit combinations is considered, all summands which correspond to the same interfering symbol have to be summed up, before applying the max-operation. This fact implies an important difference between bijective and non-bijective symbol constellations.

In this paper, an additive white Gaussian noise channel is assumed. Thus, $y = x + w$, where $w \sim \mathscr{N}(0,\sigma^2)$ is a zero-mean white Gaussian noise process with the variance σ^2. Hence, the conditional probability density function is defined as follows:

$$p(y|x) = \frac{1}{\sqrt{2\pi\sigma^2}} e^{-\frac{|y-x|^2}{2\sigma^2}}. \tag{5}$$

3. Piecewise linear detection

As visualized in Fig. 2a, for the special case without a priori information, the relation between the observation y and the corresponding extrinsic log-likelihood ratio L_n, called L–y diagram, is approximately piecewise linear. Since all modulated bits have the same influence in the DSM-EPA modulation step, the relation is the same regardless of which bit is detected. The L–y diagram is a function of the SNR. With increasing SNR, the piecewise linear approximation becomes more accurate. This fact perfectly matches to high-order modulation schemes, which naturally operate at large SNRs. The graph in Fig. 2a can roughly be divided into three main sections, namely, the two side areas and one Middle Region (MR). A more detailed view of the middle region in Fig. 2b shows that it is in fact not strictly linear, but consists of $N-1$ step-like sections. Even if a priori information is available, the two side areas and a middle region with modified step characteristics is observed. This is shown in Fig. 2c, where the a priori LLR of the interfering bits is $\mathbf{L}_A = [-5\ -5\ -5\ +5\ +5\ +5\ +5]$. For perfect a priori information, i.e., $I_A = 1$, the curve converges to a straight line. The piecewise linear characteristic is not restricted to DSM-EPA and well-known in the literature [11–18]. Due to the simple graphical characteristic representing the quite complex formula (4), the idea of piecewise linear approximation of this behavior seems to be obvious. In fact, it is sufficient to calculate a few characteristic Supporting Points (SPs), preferably the points of discontinuity, in

[4] In bijective constellations each constellation point is assigned to a unique bit tupel. In non-bijective constellations at least one constellation point is assigned to multiple bit tupels.

[5] In SISO detection the detector produces soft output values rather than hard decisions while taking soft information into account.

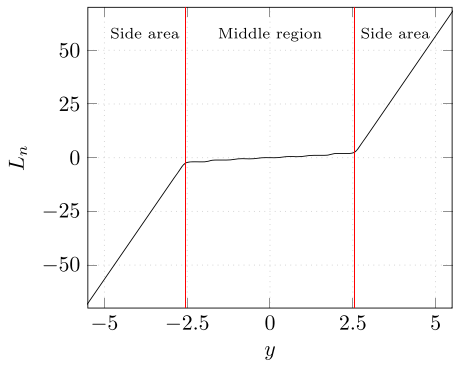

(a) No a priori information

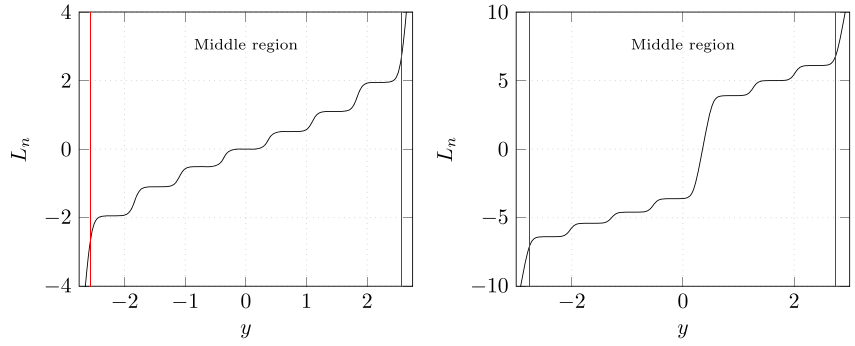

(b) No a priori information (middle region) (c) With a priori information (middle region)

Fig. 2. Relationship between extrinsic log-likelihood ratio L_n and channel observation y (N=8 layers, SNR=9 dB).

conjunction with simple linear interpolations in-between. This inherently contains potential for complexity reduction of the symbol detector in comparison to the classical APP approach. However, the calculation of the SP in the presence of a priori information is somehow difficult and complex for bijective modulation schemes like square QAM. As a result, the proposed detection algorithms in [11–18] are not practical for implementation in BICM-ID. In contrast, for DSM-EPA, as will be shown later, a complexity reduction is achieved by exploiting the non-bijective symmetric symbol constellation.

Considering DSM-EPA, in the following an algorithm is derived for calculating characteristic SPs. Afterwards, the complexity of this algorithms is analyzed. These SPs can be used for performing Piecewise Linear (PL) detection.

3.1. Approximated APP detection by means of PL detection

The main idea of identifying appropriate SPs is to approximate the two sums in (4) by their dominant summands in such a way that the formula is simplified. Towards this goal, it is constructive to distinguish between the following three scenarios:

3.1.1. Single-Term (ST)

In the first scenario, the case $y \pm \alpha \in \mathscr{Z}$ is considered. This implies that y lies exactly between two interfering symbols z, i.e., exactly on a symbol x. Hence, the squared Euclidean distance between y and $z = y - \alpha$ in the numerator of (4), as well as the squared Euclidean distance between y and $z = y + \alpha$ in the denominator, is zero. Thus, the corresponding summands are assumed to be dominant in the numerator and denominator. This leads to the following approximation of (4):

$$L_{\mathrm{ST},n} \approx \log \frac{P(z=y-\alpha)\mathrm{e}^{-\frac{|(y-\alpha)-(y-\alpha)|^2}{2\sigma^2}}}{P(z=y+\alpha)\mathrm{e}^{-\frac{|(y+\alpha)-(y+\alpha)|^2}{2\sigma^2}}} = \log \frac{P(z=y-\alpha)}{P(z=y+\alpha)}. \tag{6}$$

3.1.2. Double-Term (DT)

In the second scenario, the case $y \pm 2\alpha \in \mathscr{Z}$ is studied. This implies that y lies exactly on an interfering symbol z, and $y \pm \alpha$ lies between two interfering symbols. Hence, the squared Euclidean distance between y and $z_l = y - 2\alpha$, as well as between y and $z_c = y$, in the numerator of (4) and between y and $z_r = y + 2\alpha$, as well as y and $z_c = y$, in the denominator are minimized. Thus, the corresponding summands are assumed to be dominant in the numerator and denominator. This leads to the following approximation of (4):

$$\begin{aligned} L_{\mathrm{DT},n} &\approx \log \frac{P(z_\mathrm{l})\mathrm{e}^{-\frac{|z_\mathrm{l}-(y-\alpha)|^2}{2\sigma^2}} + P(z_\mathrm{c})\mathrm{e}^{-\frac{|z_\mathrm{c}-(y-\alpha)|^2}{2\sigma^2}}}{P(z_\mathrm{r})\mathrm{e}^{-\frac{|z_\mathrm{r}-(y+\alpha)|^2}{2\sigma^2}} + P(z_\mathrm{c})\mathrm{e}^{-\frac{|z_\mathrm{c}-(y+\alpha)|^2}{2\sigma^2}}} \\ &= \log \frac{P(z_\mathrm{l}=y-2\alpha)+P(z_\mathrm{c}=y)}{P(z_\mathrm{r}=y+2\alpha)+P(z_\mathrm{c}=y)}. \end{aligned} \tag{7}$$

3.1.3. Side-Area (SA)

In the third scenario, either $y \ll -N\alpha$ or $y \gg N\alpha$ is assumed. Hence, the squared Euclidean distance between $y \pm \alpha$ and the interfering symbol z is minimized, if $z_{\min} = -(N-1)\alpha$ (when $y \ll -N\alpha$) or $z_{\max} = (N-1)\alpha$ (when $y \gg N\alpha$). Thus, the corresponding summand in (4) is assumed to be dominant in both numerator and denominator. This leads to the following approximation of (4):

$$L_{\mathrm{SA},n} \approx \log \frac{P(z=z_{\min/\max})\mathrm{e}^{-\frac{|z_{\min/\max}-(y-\alpha)|^2}{2\sigma^2}}}{P(z=z_{\min/\max})\mathrm{e}^{-\frac{|z_{\min/\max}-(y+\alpha)|^2}{2\sigma^2}}} = \frac{2\alpha}{\sigma^2}\left(y - z_{\min/\max}\right). \tag{8}$$

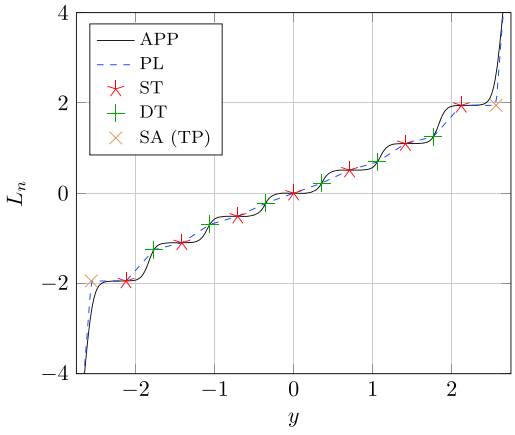

(a) No a priori information

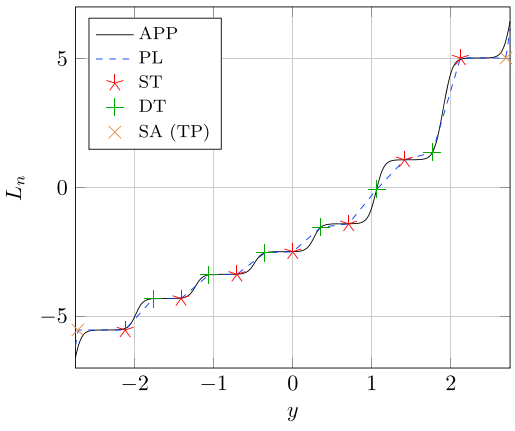

(b) With a priori information ($\mathbf{L}_A = [+5\ +4\ -5\ +2\ +3\ +3\ -1]$)

Fig. 3. Relationship between extrinsic log-likelihood ratio L_n and channel observation y for the APP approximating PL detector (N=8 layers, SNR=9 dB).

The Two Transition Points (TPs), where SA merges the middle region, is obtained by equating the right-hand sides of (6) and (8) and by solving for y:

$$y_{\mathrm{TP}} = \frac{\sigma^2}{2\alpha} L_{\mathrm{ST,min/max},n} + z_{\mathrm{min/max}} \tag{9}$$

Here, $L_{\mathrm{ST,min/max},n}$ stands for the extrinsic LLR that corresponds to the minimal/maximal ST.

With the ST, DT and SA assumption it is possible to simplify the complex equation (4). It might be surprising that the extrinsic LLR for ST and DT is independent of the noise variance and is calculated by the probability of only two or three interfering symbols. Therefore, an SNR estimation is not needed in this case. In contrast to these observations, the extrinsic LLR in SA can be calculated independent of symbol probabilities, but dependent on the noise variance. Furthermore, the position of ST and DT with respect to the y-axis do not change, even in the case that a priori information is present.

Symbol detection of an arbitrary y is done as follows: in the first step, the two nearest SPs are identified and the corresponding extrinsic LLRs are calculated by (6), (7) or (8). Afterwards, the approximated extrinsic LLR of y is obtained by simple linear interpolation between these two ratios. In the case that y is equivalent to an SP, the extrinsic LLR of this SP is directly used as soft-output. In Fig. 3, two exemplary L–y diagrams of the PL detector for both cases, with and without a priori information, are shown. Furthermore, the corresponding SPs (ST, DT, and TP of SA) are marked. It can be seen that the PL detector provides an approximation of the APP detector. The quality of the approximation is analyzed in Section 4.

3.2. Zero bound

The assumptions made in Section 3.1 are not suitable for the whole range of a priori LLRs. Especially in the case of large a priori information, the PL detector would only reach poor performance. This can be made clear when reconsidering the assumptions of ST in Section 3.1.1.

Because of the zero-distance between $y-\alpha$ and $z=y-\alpha$ in the numerator in (4), the interfering symbol $z=y-\alpha$ is assumed to be dominant. To be more precise, only the conditional probability $p(y|z, c_n=+\alpha_n)$ is considered. However, this assumption is only correct as long as the following inequality is fulfilled:

$$P(z=y-\alpha)p(y|z=y-\alpha) > P(z\neq y-\alpha)p(y|z\neq y-\alpha). \tag{10}$$

The conditional probabilities stay constant over all iterations, but the symbol probabilities change. Some of the interfering symbols may get very unlikely over iterations and therefore (10) is no longer fulfilled. Consequently, the SPs are no longer suitable, which results in poor performance.

To avoid this limitation, a Zero Bound (ZB) θ is introduced. The bound defines the smallest probability $P(z)$ that is needed for an interfering symbol to be considered in the algorithm. If $P(z)$ is less than θ, the interfering symbol is simply neglected for SP calculations, which also guarantees numerical stability of (6) and (7) for $0<\theta\leq 1$.

3.3. Max-log APP detection by means of PL detection

The main principle of the PL algorithm is exploited to achieve max-log APP performance exactly. It is well-known that the max-log APP algorithm leads to a piecewise linear approximation of the APP detector. But instead of applying the max-function in (4), the PL algorithm is used to determine the corresponding SPs, even if a priori information is present. Due to applying the max-function in (4), only one interfering symbol in the numerator and denominator is considered. Thus, there are two different scenarios to distinguish between.

The first one is similar to the ST introduced in Section 3.1.1. In that case, the dominant interfering symbols in the numerator and denominator are not equal, but two neighbors z_l and $z_r = z_l + 2\alpha$. Thus, the extrinsic LLR of this SP can also be calculated by (6) and is independent of the noise variance:

$$L_{\mathrm{SP},n} \approx \log\frac{P(z_l)}{P(z_r)}. \tag{11}$$

The second scenario is similar to the SA introduced in Section 3.1.3. In that case, the dominant interfering symbols in the numerator and denominator are equal. In contrast to the previous definition, SA is here also allowed to be inside MR. Thus, (8) is extended to:

$$L_{\mathrm{SA},n} \approx \frac{2\alpha}{\sigma^2}\left(y - z_{l/r}\right). \tag{12}$$

The SP, where the two scenarios merge, is obtained by equating the right-hand sides of (11) and (12) and by solving for y:

$$y_{\mathrm{SP,l},n} = \frac{\sigma^2}{2\alpha} L_{\mathrm{SP},n} + z_l \tag{13}$$

$$y_{\mathrm{SP,r},n} = \frac{\sigma^2}{2\alpha} L_{\mathrm{SP},n} + z_r = y_{\mathrm{SP,l},n} + 2\alpha. \tag{14}$$

For symbol detection of an arbitrary y, the extrinsic LLRs of relevant SPs have to be calculated by (11). Afterwards, the corresponding SPs are

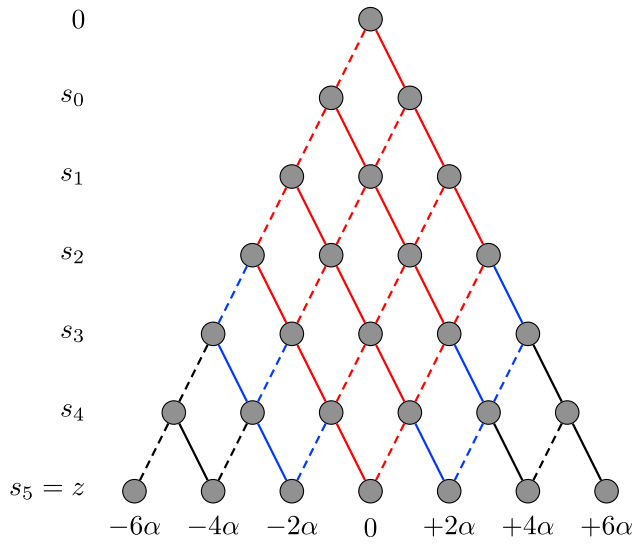

Fig. 4. Tree representation of the interfering symbols for DSM-EPA with N=7 layers.

obtained by (13) and (14). In the last step, the final extrinsic LLR is determined by simple linear interpolation between the SPs.

3.4. Complexity

The main complexity of the PL detection comes from the calculation of the probabilities $P(z)$ of the interfering symbols. Notice that the position of the ST and DT do not change with respect to the y-axis, even if a priori information is taken into account. Thus, a search in each iteration for the corresponding dominant interfering symbols is not necessary. A big advantage of DSM-EPA over other modulation schemes is the fact that the modulation-step can be visualized by a tree diagram [9], as it is shown in Fig. 4 for the case of DSM-EPA with N=7 layers. This can be exploited when determining $P(z)$, because the probabilities are calculated along the branches. Hence, the complexity is proportional to the amount of branches that are necessary for determining $P(z)$. Therefore, the number of required branches is analyzed in the following. For completeness a detailed complexity analysis by means of required basic operations (max-operations, if conditions, additions/subtractions, multiplications, exponential/logarithmic function, and table look-ups) is given in Table 1. Depending on y it is possible to distinguish between different scenarios that result in different complexities.

In the simplest case, y lies in SA. According to (8), it is not necessary to calculate any probabilities. In fact it is sufficient to solve this linear equation, which is simply implemented via an LUT. Thus, the complexity for this case is assumed to be negligibly small.

In the worst case, N is odd and y lies between the middle DT y_{DT} and the ST y_{ST}. Thus, $P(z)$ of three different interfering symbols, namely $P(z = y_{\mathrm{DT}})$ and $P(z = y_{\mathrm{DT}} \pm 2\alpha)$ including $P(z = y_{\mathrm{ST}} \pm \alpha)$, have to be determined for solving (6) and (7). Since y_{DT} is the middle DT, the amount of branches needed for calculation of $P(z = y_{\mathrm{DT}})$ is equal to $(N^2 - 1)/2$. In Fig. 4, these branches are represented by the red lines. The branches from determining $P(z = y_{\mathrm{DT}})$ are reused when calculating $P(z = y_{\mathrm{DT}} \pm 2\alpha)$. Hence, additionally $2N - 4$ branches are necessary, which are represented by the blue lines in Fig. 4. This leads to a total amount of $N^2/2 + 2N - 9/2$ branches and thus to a complexity of $\mathcal{O}(N^2)$. For the PL max-log APP algorithm, analogous considerations lead to a minimum complexity of just one table look-up and a maximum complexity of $\mathcal{O}(N^2)$ as well. Hereby, the worst case appears when N is odd and y lies in the SA between the two central ST.

Compared to classical APP and max-log APP detectors which imply a complexity of $\mathcal{O}(2^{N'})$, the proposed PL detection algorithms inherently reduce the complexity, even in a worst case scenario and even if a priori information is present. An efficient detection is performed in the first iteration, where no a priori information exists at the receiver input. Due to the fact that the behavior of extrinsic LLRs over all channel observations is the same, regardless of which modulated bit should be detected, the whole detector is implemented via one LUT.

4. Simulation results

In this section, numerical results will be provided for the detectors introduced in the previous two sections. Specifically, an Extrinsic Information Transfer (EXIT) chart analysis [19] and Bit Error Rate (BER) measurements are conducted. The presented simulation results are performed for high-order DSM-EPA with N=8 layers (corresponding to $N' = 2N = 16$ layers for the complex symbol). Our target is a bandwidth efficiency of 2 bits/symbol/dimension (corresponding to 4 bits/complex-valued symbol). For Gaussian distributed channel inputs, the corresponding channel capacity is obtained at 8.75 dB. With regard to Fig. 5, an operating point of SNR=9 dB is chosen for the code design, because it exhibits the target bandwidth efficiency while still maintaining the capacity achieving behavior of DSM-EPA. Because real and imaginary symbol parts are modulated independently, the detection is performed separately for each component. Thus, without loss of generality, only the detection of the real part is examined in the simulations. Since the PL max-log APP detector achieves exactly max-log APP performance, it is excluded from the simulation results.

4.1. EXIT chart analysis

Fig. 6 shows the EXIT charts for the APP, max-log APP and PL detector, respectively, for the defined simulation parameters. For each detector, 100,000 symbols were processed with a priori information given a resolution of 0.02. The transfer characteristics do not terminate in the ideal point (1,1). This causes an error floor in the BER simulations. However, the (1,1) point is approached by code doping [20], which reduces or even avoids the error floor. Anyway, the main focus in this paper is on low-complexity detection rather than on error floor removal, so code doping is beyond the scope of this contribution. The different

Table 1
Complexity analysis per quadrature component and bit between the conventional (max-)log APP algorithm and the proposed PL detection algorithms, taken into account the additional complexity of including a priori information. Concerning the PL APP / PL max-log APP, SC refers to the simplest case and WC to the worst case, as explained in the text.

Operation	Log APP	Max-log APP	PL APP		PL max-log APP	
			SC	WC	SC	WC
MAX	$2^N + N$	$2^N + N$	0	0	0	0
IF	$(N+1) \times 2^N$	$(N+1) \times 2^N$	0	0	0	4
ADD/SUB	$\left(N + 2 + \frac{2}{N}\right) \times 2^N + 2N + 2$	$\left(N + 1 + \frac{2}{N}\right) \times 2^N + 2N + 2$	0	$\frac{N^2+10N+9}{4}$	0	$\frac{N^2+10N-11}{4}$
MULT	$\frac{5}{N} \times 2^N$	$\frac{5}{N} \times 2^N$	0	$\frac{N^2+6N-11}{2}$	0	$\frac{N^2+6N-15}{2}$
EXP/LOG	0	0	0	$N+3$	0	$N+3$
LUT	$2^N + N$	N	1	0	1	5

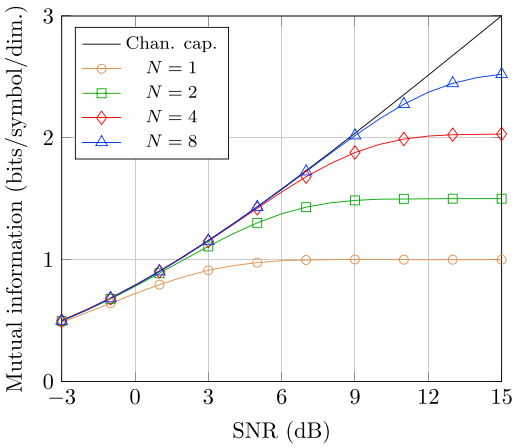

Fig. 5. Mutual information versus SNR for DSM-EPA with different number of layers N.

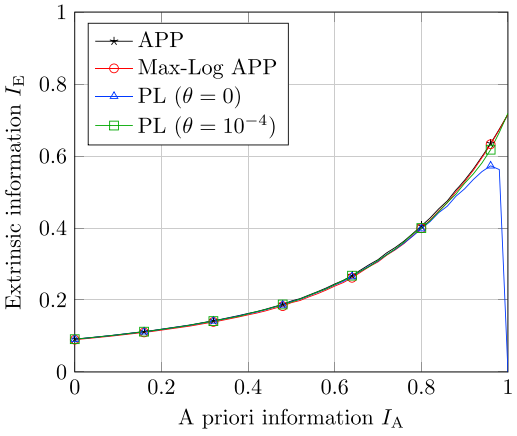

Fig. 6. EXIT chart of different detectors for DSM-EPA (N=8, SNR=9 dB).

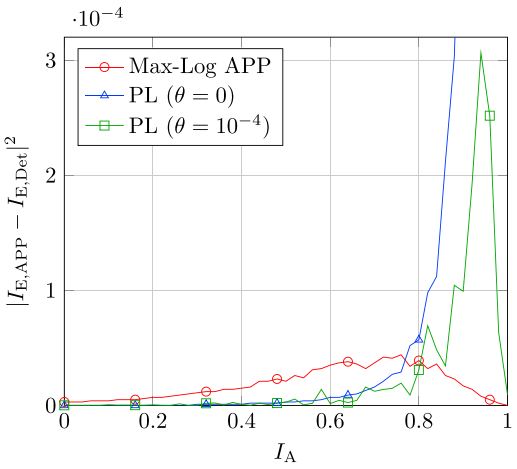

Fig. 7. Quadratic error of different detectors with respect to APP performance in the EXIT chart (Fig. 6).

transfer curves in Fig. 6 show nearly the same behavior when disregarding large I_A values. The reason for the performance loss of the pure PL detector is described in Section 3.2 and is solved by introducing a ZB. For a better performance analysis, the quadratic error in the EXIT chart of the detectors to the optimal APP detector is depicted in Fig. 7. It can be seen that the PL detector can outperform the max-log APP detector in the EXIT chart. For large I_A values, the ZB is used to improve the performance of the PL detector. There exists a trade-off in the choice of θ. A decreasing ZB leads to a better performance for small and a worse performance for large I_A values, while an increasing ZB gives a worse performance for small and a better performance for large I_A values. For the scenario under investigation, we have optimized θ numerically over the interval $\theta = 10^{-i}$ with $i \in [0, \ldots, 6]$. The optimum is in between $\theta = 10^{-3}$ and $\theta = 10^{-4}$, therefore the ZB is chosen to be $\theta = 10^{-4}$. The parameter θ is independent of the channel code. A theoretical analysis of how to determine the optimal θ is considered as future work.

4.2. BER simulation

For BER simulations, a suitable channel code has to be applied for BICM-ID. According to Fig. 5, theoretically a bandwidth efficiency of 2 bits/symbol/ dimension can be achieved at SNR=9 dB (corresponding to SNR=12 dB for complex-valued symbols). Hence, a code with a rate $R = 1/4$ is necessary when using DSM-EPA with N=8 layers. In order to achieve near-capacity performance (at least for APP detection) without active signal shaping, an irregular convolutional code,[6] according to [21] and with a code rate of about $R \approx 1/4$, has been matched by means of an EXIT chart design to DSM-EPA employing N=16 layers, cf. Table 2. The related EXIT chart of the APP detector and the IRCC decoder is visualized in Fig. 8. The small gap between the transfer characteristics of the detector and decoder promotes the desired bandwidth efficiency. For BER simulations an information word length of 100, 000 bits has been chosen and 500 global iterations have been performed.

Table 2
Parameter set of the irregular convolutional code used in the simulation results. The subcodes are obtained from a recursive systematic convolutional code by puncturing and repetitions, respectively. The code polynomials and the puncturing/repetition table are given in [21].

j	R_j	α_j
1	0.10	0.254042
2	0.15	0.292594
3	0.20	0.003651
4	0.25	0.133594
5	0.30	0.054518
6	0.35	0.032276
7	0.40	0.092666
8	0.45	0.000000
9	0.50	0.000000
10	0.55	0.105838
11	0.60	0.030820

Fig. 9 shows the BER simulation results. All detectors cause the same error floor, which can be reduced or avoided by means of code doping [20] (as indicated by the dashed lines), but this is not the focus of this paper. For the APP detector, the turbo cliff in Fig. 9 is at about 9.5 dB, which corresponds to a gap of approximately 0.75 dB with respect to the theoretical limit of 8.75 dB. In comparison to the shaping loss of 1.53 dB when using ASK, this result provides significant improvements. The overall loss of about 0.75 dB can be divided into two parts. The first part is due to the DSM modulation scheme itself. As shown in Fig. 5, there is a small gap of about 0.25 dB with respect to channel capacity at the target bandwidth efficiency. The second part corresponds to the remaining loss of

[6] An irregular convolutional code C of rate R consists of J punctured convolutional codes C_j of rates R_j implemented in parallel, where $R = \sum_{j=1}^{J} \alpha_j R_j$ and $\sum_{j=1}^{J} \alpha_j = 1$. The EXIT chart characteristic of the irregular convolutional code can be shaped by optimizing the parameter set α_j, $1 \le j \le J$.

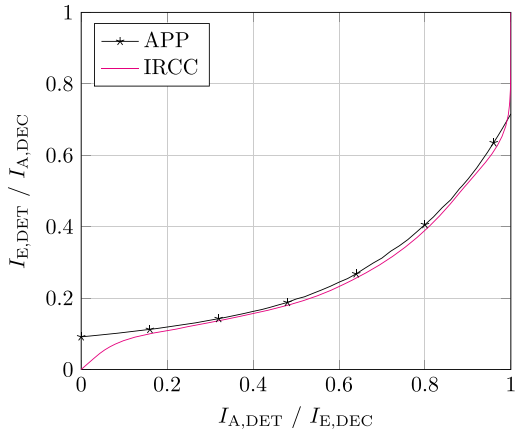

Fig. 8. EXIT chart of APP detector for DSM-EPA and $R \approx 0.25$ IRCC (N=8, SNR=9 dB).

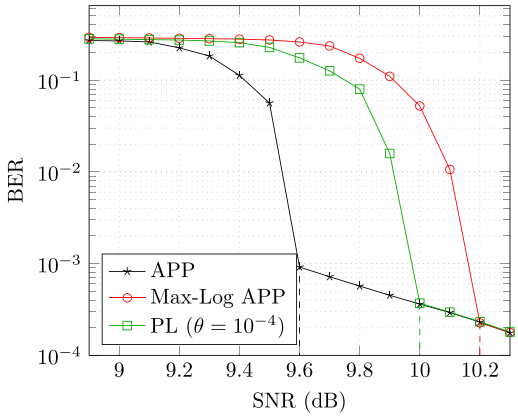

Fig. 9. Bit error rate performance (N=8).

approximately 0.5 dB. This is partly due to imperfections, e.g., the finite number of iterations and a finite interleaver depths. Additionally, the selected IRCC code is not optimal, because the tunnel area in Fig. 8 is not zero.

In Fig. 9, the PL detector degrades about 0.37 dB, while the max-log APP detector degrades about 0.56 dB compared to the APP detector in the area of the turbo cliff. Naturally, there is a loss due to the approximation process, but one additional degrading factor is the fact that the selected IRCC has neither been optimized for the PL detector nor for the max-log APP detector. Yet, the BER simulation results confirm two main hypotheses: the first one is the near-capacity achieving behavior of DSM-EPA without active signal shaping, and the second and most important one is the fact that the PL detector typically outperforms the max-log APP detector.

5. Conclusion

The bottleneck of high-order digital modulation schemes is the complexity of soft-output detection. Classically, APP detection (or a simplification thereof) is performed in iterative receivers in order to exchange extrinsic information between constituent detectors/decoders. This paper is motivated by the well-known fact that the soft outputs delivered by the APP detector or the max-log APP detector are well approximated by a piecewise linear function of the detector input samples, as demonstrated in [11–18] for ASK and square QAM in the absence of a priori information. For DSM-EPA, it is shown in this paper that the discontinuity points of this function are easily computed off-line, even if a priori knowledge about the modulated bits is available. The points of discontinuity are stored in a look-up table, and interpolation is performed in-between. Due to the piecewise approximately linear detector characteristic, computational complexity is inherently reduced with a small performance loss. Even for on-line computation the proposed detection algorithm achieves a complexity of $\mathcal{O}(N^2)$ at most. Hence, high-order modulation schemes can be implemented efficiently in conjunction with BICM-ID. Specifically, it is demonstrated that at least max-log APP performance is reached. A generalization of the main principle towards modulation schemes which cannot be split into real and imaginary part is a subject for future work. Furthermore, it would be interesting to identify other classes of modulation schemes, where a piecewise approximated linear detection provides a low-complexity detection, even if a priori information is taken into account. A generalization towards related detection problems like trellis-based equalization, multiuser detection, and multiple-input multiple-output detection should also be investigated.

Acknowledgment

This work has partly been funded by the German Research Foundation (DFG) under Contract no. HO2226/14-1.

References

[1] G. Caire, G. Taricco, E. Biglieri, Bit-interleaved coded modulation, IEEE Trans. Inf. Theory 44 (3) (1998) 927–946, https://doi.org/10.1109/18.669123.
[2] S. ten Brink, J. Speidel, R.-H. Yan, Iterative demapping and decoding for multilevel modulation, in: Proceedings of IEEE Global Communications Conference (GLOBECOM), 1998, pp. 579–584.
[3] L. Bahl, J. Cocke, F. Jelinek, J. Raviv, Optimal decoding of linear codes for minimizing symbol error rate, IEEE Trans. Inf. Theory 20 (2) (1974) 284–287, https://doi.org/10.1109/TIT.1974.1055186.
[4] J. Erfanian, S. Pasupathy, P. Gulak, Reduced complexity symbol detectors with parallel structure for ISI channels, IEEE Trans. Commun. 42 (234) (1994) 1661–1671, https://doi.org/10.1109/TCOMM.1994.582868.
[5] P. Robertson, P.A. Hoeher, E. Villebrun, Optimal and sub-optimal maximum a posteriori algorithms suitable for turbo decoding, Eur. Trans. Telecommun. 8 (2) (1997) 119–125.
[6] L. Ping, L. Liu, W.K. Leung, A simple approach to near-optimal multiuser detection: interleave-division multiple-access, in: Proceedings of IEEE Wireless Communications and Networking Conference (WCNC), vol. 1, New Orleans, USA, 2003, pp. 391–396. https://doi.org/10.1109/WCNC.2003.1200381.
[7] P.A. Hoeher, Adaptive interleave-division multiple access – a potential air interface for 4G bearer services and wireless LANs, in: Proceedings of IEEE and IFIP International Conference on Wireless and Optical Communications and Networks (WOCN), Muscat, Oman, 2004, pp. 179–182.
[8] M. Noemm, T. Wo, P.A. Hoeher, Multilayer APP detection for IDM, Electron. Lett. 46 (1) (2010) 96–97, https://doi.org/10.1049/el.2010.1755.
[9] P.A. Hoeher, T. Wo, Superposition modulation: myths and facts, IEEE Commun. Mag. 49 (12) (2011) 110–116, https://doi.org/10.1109/MCOM.2011.6094014.
[10] X. Ma, L. Ping, Coded modulation using superimposed binary codes, IEEE Trans. Inf. Theory 50 (12) (2004) 3331–3343, https://doi.org/10.1109/TIT.2004.838104.
[11] F. Tosato, P. Bisaglia, Simplified soft-output demapper for binary interleaved COFDM with application to HIPERLAN/2, in: Proceedings of IEEE International Conference on Communications (ICC), vol. 2, 2002, pp. 664–668.
[12] K. Hyun, D. Yoon, Bit metric generation for Gray coded QAM signals, in: IEE Proceedings – Communications, vol. 152, no. 6, 2005, pp. 1134–1138.
[13] M. Raju, R. Annavajjala, A. Chockalingam, BER analysis of QAM on fading channels with transmit diversity, IEEE Trans. Wirel. Commun. 5 (3) (2006) 481–486.
[14] A. Alvarado, L. Szczecinski, R. Feick, L. Ahumada, Distribution of L-values in gray-mapped M2-QAM: closed-form approximations and applications, IEEE Trans. Commun. 57 (7) (2009) 2071–2079.
[15] R. Yazdani, M. Ardakani, Efficient LLR calculation for non-binary modulations over fading channels, IEEE Trans. Commun. 59 (5) (2011) 1236–1241.
[16] R. Asvadi, A. Banihashemi, M. Ahmadian-Attari, H. Saeedi, LLR approximation for wireless channels based on Taylor series and its application to BICM with LDPC codes, IEEE Trans. Commun. 60 (5) (2012) 1226–1236.

[17] G. Baruffa, L. Rugini, Soft-output demapper with approximated LLR for DVB-T2 systems, in: Proceedings of IEEE Global Communications Conference (GLOBECOM), 2015, pp. 1–6.
[18] M. Sandell, F. Tosato, A. Ismail, Low complexity max-log LLR computation for nonuniform PAM constellations, IEEE Commun. Lett. 20 (5) (2016) 838–841.
[19] S. Ten Brink, Convergence of iterative decoding, Electron. Lett. 35 (10) (1999) 806–808, https://doi.org/10.1049/el:19990555.
[20] S. Pfletschinger, F. Sanzi, Error floor removal for bit-interleaved coded modulation with iterative detection, IEEE Trans. Wirel. Commun. 5 (11) (2006) 3174–3181, https://doi.org/10.1109/TWC.2006.05163.
[21] M. Tuechler, Design of serially concatenated systems depending on the block length, IEEE Trans. Commun© 2017 Chongqing University of Posts and Telecommunications. Production and hosting by Elsevier B.V. This is an open access article under the CC BY-NC-ND license (http://creativecommons.org/licenses/by-nc-nd/4.0/).. 52 (2) (2004) 209–218.